Received: 19 May 2025 | Revised: 24 June 2025 | Accepted: 27 June 2025

DOI: 10.1002/pro.70227

RESEARCH ARTICLE

THE PROTEIN SOCIETY WILEY

Structure–function relationship of the *Pseudomonas aeruginosa* AsmA-like proteins YhdP and YdbH involved in outer membrane biogenesis

Davide Sposato[1] | **Camilla Pederzoli**[1] | **Marianna Bufano**[2] | **Pietro Sciò**[2] | **Ludovica Rossi**[1] | **Livia Leoni**[1] | **Giordano Rampioni**[1,3] | **Paolo Visca**[1,3,4] | **Antonio Coluccia**[2] | **Francesco Imperi**[1,3,4]

[1]Department of Science, University Roma Tre, Rome, Italy

[2]Department of Drug Chemistry and Technologies, Sapienza University of Rome, Rome, Italy

[3]IRCCS Fondazione Santa Lucia, Rome, Italy

[4]NBFC, National Biodiversity Future Center, Palermo, Italy

Correspondence
Francesco Imperi, Viale Guglielmo Marconi 446, 00146 Rome, Italy.
Email: francesco.imperi@uniroma3.it

Funding information
Rome Technopole, Grant/Award Number: F83B22000040006; Ministero dell'Università e della Ricerca, Grant/Award Numbers: PRIN 2020 (20208LLXEJ), PRIN 2022 (20224BYR59/2022C5PNXB); National Biodiversity Future Center, Grant/Award Number: CN00000033; Fondazione per la Ricerca sulla Fibrosi Cistica, Grant/Award Number: FFC#6/2023

Review Editor: Aitziber L. Cortajarena

Abstract

The outer membrane (OM) of Gram-negative bacteria is an asymmetric bilayer composed of glycerophospholipids (GPLs) in the inner leaflet and lipopolysaccharide in the outer leaflet, which is critical for viability and antibiotic resistance. While the mechanisms for lipopolysaccharide and OM protein transport across the periplasm are well characterized, it has only recently been proposed that AsmA-like proteins are likely involved in the anterograde transport of GPLs. Here, we investigated the structural and functional features of *Pseudomonas aeruginosa* YhdP, an AsmA-like protein that exhibits higher activity in maintaining OM integrity than its paralogs. Through structural predictions, molecular dynamics simulations, and genetic complementation assays, we demonstrated that two hydrophobic α-helices at the C-terminal region of YhdP are crucial for its function. Moreover, we found that fusing the YhdP C-terminal domain to YdbH enhances the functionality of this shorter and lower-activity AsmA-like protein. Specifically, a YdbH-YhdP fusion protein long enough to potentially span the periplasmic space was more active than the wild-type YdbH protein in promoting growth and OM integrity. Furthermore, while YdbH activity requires the OM protein partner YnbE, the functionality of the YdbH-YhdP fusion protein is YnbE-independent. These findings support the hypothesis that the YhdP C-terminus provides OM anchoring and likely assists GPL insertion, and prove that it can be used as a modular element for improving the activity of other AsmA-like proteins. Our work sheds light on the molecular determinants of GPL transport and offers a framework for studying the mode of action of AsmA-like proteins in OM biogenesis.

KEYWORDS

anterograde transport, *Escherichia coli*, glycerophospholipids, Gram-negative bacteria, hybrid proteins, molecular dynamics simulations, outer membrane integrity, periplasm, *Pseudomonas aeruginosa*, structure–function relationship

1 | INTRODUCTION

The tripartite cell envelope of Gram-negative bacteria consists of the cytoplasmic/inner membrane (IM), a periplasmic space containing a thin peptidoglycan cell wall, and the outer membrane (OM) (Silhavy et al., 2010). While the IM is a typical glycerophospholipid (GPL) bilayer, the OM is an asymmetric bilayer made of GPLs in the inner leaflet and lipopolysaccharide (LPS) in the outer leaflet, which also accommodates numerous integral OM proteins (OMPs) and lipoproteins (Henderson et al., 2016).

The OM is an essential structure of Gram-negative bacteria that provides mechanical strength and protection from large and/or hydrophobic toxic molecules, including many antibiotics, partly explaining the intrinsic drug resistance of Gram-negative pathogens (Nikaido, 2003; Sun et al., 2022). Understanding the composition and biogenesis of the OM remains a crucial area of research, as it holds potential for identifying novel drug targets and developing new antibacterials (Choi & Lee, 2019; Sperandeo et al., 2023; Walker & Black, 2021). Disrupting OM biogenesis can indeed directly lead to bacterial cell death or increase susceptibility to antimicrobials that would otherwise be ineffective due to the OM permeability barrier (Lehman & Grabowicz, 2019; Wesseling & Martin, 2022).

The assembly of the OM requires the transport of several hydrophobic molecules across the aqueous periplasmic space, which occurs through specialized protein transport systems. Lipoproteins and OMPs are translocated and inserted into the OM by the Lol and Bam systems, respectively, which use soluble carrier proteins to shuttle their substrates across the periplasm (Plummer & Fleming, 2016; Zückert, 2014). LPS is transported to the OM as a continuous stream through the Lpt system, a periplasm-spanning protein complex that bridges the IM and the OM (Okuda et al., 2016; Sperandeo et al., 2019). On the other hand, the mechanism by which GPLs are translocated across the periplasm and inserted into the OM (anterograde GPL transport) remained elusive for decades. However, recent studies performed in *Escherichia coli* and *Pseudomonas aeruginosa* provided indirect genetic and biochemical evidence that members of the AsmA-like protein family are likely responsible for this process (Cooper et al., 2025; Douglass et al., 2022; Grimm et al., 2020; Rai et al., 2024; Ruiz et al., 2021; Sposato et al., 2024). Specifically, three AsmA-like proteins (YhdP, TamB, and YdbH) were found to be essential yet redundant in *E. coli* (Ruiz et al., 2021), and four in *P. aeruginosa* (YhdP, TamB, YdbH, and PA4735/EpaF) (Sposato et al., 2024) (Figure 1a). Moreover, the depletion of these proteins resulted in defective phenotypes consistent with impaired GPL transport from the IM to the OM, which could be partly rescued by restoring the asymmetry of the OM through chemical or genetic inhibition of LPS transport (Douglass et al., 2022; Ruiz et al., 2021; Sposato et al., 2024). Very recently, Cooper and collaborators provided the first evidence that one of these proteins, *E. coli* YhdP, interacts in vivo with phosphate-containing molecules, likely GPLs (Cooper et al., 2025).

Bacterial AsmA-like proteins are characterized by an N-terminal transmembrane α-helix (TMH), which anchors them to the IM, and a large soluble domain predicted to span into the periplasm, which contains a Chorein-N domain followed by an AsmA-like domain of variable length (Kumar & Ruiz, 2023; Levine, 2019). These proteins share structural similarity with eukaryotic proteins, such as Vps13 and Atg2, that mediate lipid transfer between organelles (Kumar and Ruiz 2023; Lees & Reinisch, 2020; Levine, 2019; Melia & Reinisch, 2022), suggesting a conserved role in intermembrane lipid transport. Structural predictions from AlphaFold indicate that AsmA-like proteins form extended, tube-like structures consisting of stacked β-strands, which create a continuous hydrophobic groove along the long axis (Cooper et al., 2025; Douglass et al., 2022; Ruiz et al., 2021; Sposato et al., 2024). Such a groove is reminiscent of that formed by the β-jellyroll domains of Lpt proteins in the periplasm, which accommodate LPS during transport from the IM to the OM (Dong et al., 2017; Hicks & Jia, 2018), supporting the hypothesis that AsmA-like proteins may work as protein bridges for GPL translocation across the periplasm.

While a single AsmA-like protein associated with GPL transfer is sufficient to support bacterial growth, highlighting redundant functions, in both *E. coli* and *P. aeruginosa*, the absence of YhdP causes more relevant defects in OM integrity as compared to the lack of other AsmA-like proteins (Ruiz et al., 2021; Sposato et al., 2024). YhdP is the only AsmA-like protein whose length seems sufficient to span the periplasm (Cooper et al., 2025; Ruiz et al., 2021; Sposato et al., 2024), and molecular dynamics simulations suggested that its C-terminus may interact with the OM, thus supporting its possible envelope spanning nature (Cooper et al., 2025). In contrast, other AsmA-like proteins are predicted to be either too twisted (TamB) or too short (YdbH and PA4735) to cross the entire periplasmic space (Kumar & Ruiz, 2023; Ruiz et al., 2021; Sposato et al., 2024). Accordingly, TamB interacts with the OM β-barrel protein TamA (Selkrig et al., 2015), and this interaction was found to be required for the function of TamB in maintaining OM homeostasis in both *E. coli* and *P. aeruginosa* (Ruiz et al., 2021, Sposato et al., 2024). Recently, it has also been shown that the *E. coli* protein YdbH forms a functional complex with the OM lipoprotein YnbE, which extends the continuous hydrophobic groove of YdbH and is important for its functionality (Kumar et al., 2024).

Using *P. aeruginosa* AsmA-like proteins as a model system, in this study we aimed to elucidate the structural/biochemical features of YhdP that account for its apparently higher efficiency in supporting OM functionality and,

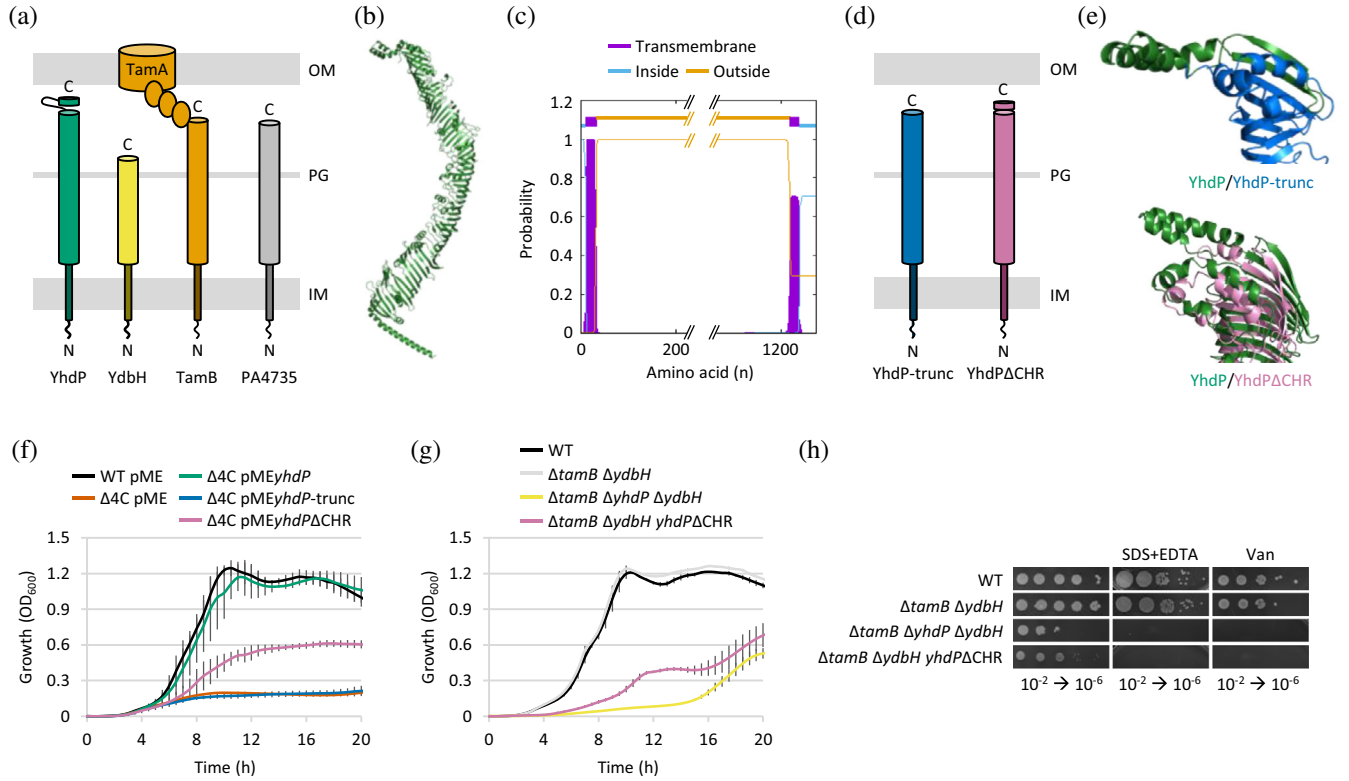

FIGURE 1 (a) Schematic representation of the *Pseudomonas aeruginosa* AsmA-like proteins that are essential but redundant for growth and OM integrity. (b) Predicted 3D structure of *P. aeruginosa* YhdP. (c) Putative TMHs in *P. aeruginosa* YhdP predicted by TMHMM 2.0. (d) Schematic representation of the *P. aeruginosa* YhdP variants lacking the C-terminal domain (YhdP-trunc) or only the C-terminal hydrophobic residues (YhdPΔCHR). (e) Superimposition of the predicted structures of the C-terminal domain of *P. aeruginosa* YhdP and the variant YhdP-trunc (upper panel) or YhdPΔCHR (lower panel). (f) Growth curves of the wild-type strain *P. aeruginosa* PAO1 (WT) and the rhamnose-dependent conditional mutant Δ*tamB* Δ*yhdP* Δ*ydbH rhaSR*-P_{rhaBAD}::*tamB* ΔPA4735 (Δ4C) carrying the empty plasmid pME6032 (pME) or its derivatives for IPTG-inducible expression of YdbH, YhdP-trunc, or YhdPΔCHR, cultured in Mueller Hinton broth (MH) supplemented with 125 μM IPTG. Growth curves of the same strains at different IPTG concentrations are shown in Figure S2. (g) Growth curves of PAO1 (WT) and the isogenic mutants Δ*tamB* Δ*ydbH*, Δ*tamB* Δ*yhdP* Δ*ydbH*, and Δ*tamB* Δ*ydbH yhdP*ΔCHR cultured in MH. (h) Plating efficiency of the same strains described in panel G on MH agar plates supplemented or not with 0.25% SDS and 0.25 mM EDTA (SDS + EDTA) or 100 μg/mL vancomycin (Van). Data in panels f–g are the mean (±standard deviation) of three independent experiments. Images in panel H are representative of three independent experiments. IM, inner membrane; OM, outer membrane; PG, peptidoglycan.

presumably, GPL transport or insertion into the OM. By generating and expressing mutant YhdP variants and YdbH-YhdP fusion proteins, we demonstrated that two hydrophobic α-helices in the C-terminal region of YhdP are crucial for its function. Moreover, the YhdP C-terminal domain can confer to YdbH higher activity and the ability to function independently of its OM protein partner YnbE, provided that the fusion protein is long enough to potentially span the periplasmic space.

2 | RESULTS AND DISCUSSION

2.1 | Hydrophobic α-helices at the C-terminus are crucial for *P. aeruginosa* YhdP function

Alpha-fold structural prediction suggested the presence of two putative α-helices in the C-terminal region of *P. aeruginosa* YhdP (Figure 1b). These α-helices contain several hydrophobic residues and are indeed predicted as a possible TMH by the transmembrane prediction software TMHMM 2.0, spanning residues 1220–1239 (Figure 1c). Similar C-terminal hydrophobic regions are not present in any other *P. aeruginosa* AsmA-like protein (data not shown), suggesting that this may represent a unique feature of YhdP. Notably, analogous C-terminal hydrophobic α-helices were recently identified in the YhdP ortholog of *E. coli* and shown to be required for its function (Cooper et al., 2025).

To confirm that such C-terminal region is also important for the *P. aeruginosa* YhdP protein, we generated plasmid constructs to express two YhdP variants lacking either the entire C-terminal region (residues 1220–1276) or only the two predicted α-helices (residues 1216–1241). These variants were named YhdP-trunc and YhdPΔCHR (C-terminal hydrophobic residues),

respectively (Figure 1d; Table S1). Structural predictions suggested that these deletions are unlikely to disrupt the overall folding of the YhdP tubular domain (Figure 1e). To assess their structural stability and confirm that they retain proper folding and domain organization, we performed extensive coarse-grained molecular dynamics simulations (Joshi & Deshmukh, 2021), comparing their trajectories to those of the wild-type protein (Figure S1). Structural stability was evaluated using three key metrics: (i) the radius of gyration, to monitor global compactness and folding consistency; (ii) the fraction of native contacts (Best et al., 2013), to assess preservation of the native tertiary structure; (iii) the level of frustration, as a measure of the energetic conflict in the folded proteins (Onuchic et al., 1997; Vannimenus & Toulouse, 1977). All three metrics indicated that the studied proteins remained structurally stable throughout the simulations. Radius of gyration values remained consistent over time, showing no significant fluctuations. The fraction of native contacts remained high ($Q > 0.9$) for all models, confirming retention of overall structural integrity. Analysis of local frustration revealed comparable energetic profiles between the chimeric variants and the wild-type protein, with no increase in destabilizing interactions (Figure S1). Together, these results suggest that the chimeric proteins are intrinsically stable, supporting the accuracy of the modeled structures and their potential to maintain native-like functional behavior.

These YhdP variants were expressed in the *P. aeruginosa* conditional mutant Δ*tamB* Δ*yhdP* Δ*ydbH rhaSR*-P_{rhaBAD}::*tamB* ΔPA4735 (Sposato et al., 2024), which lacks *yhdP*, *ydbH*, and PA4735, and expresses *tamB* from a rhamnose-inducible promoter. As expected, ectopic expression of wild-type YhdP restored the growth of the conditional mutant to wild-type levels in the absence of rhamnose (Figure 1f), confirming that YhdP alone is sufficient to efficiently support *P. aeruginosa* growth (Sposato et al., 2024). In contrast, expression of YhdP-trunc had no effect on the growth profile of the conditional mutant, while expression of YhdPΔCHR partially promoted the growth of the conditional mutant; however, it did not allow to reach the levels of the wild-type control strain (Figure 1f).

In order to assess the growth-promoting effect of YhdPΔCHR when expressed at physiological levels, we compared the growth profile of the triple mutant Δ*tamB* Δ*yhdP* Δ*ydbH* to that of the double mutant Δ*tamB* Δ*ydbH* carrying a mutated *yhdP* allele for expression of the YhdPΔCHR variant. The double mutant expressing YhdPΔCHR exhibited minimal growth improvement compared to the triple mutant lacking YhdP (Figure 1g). Moreover, both the absence of YhdP and the expression of YhdPΔCHR in TamB- and YdbH-deficient cells caused extreme sensitivity to agents that disrupt the membranes (SDS and EDTA) or to an antibiotic that is poorly active against Gram-negative cells with an intact OM (vancomycin) (Figure 1h), indicating that YhdPΔCHR is not able to restore OM integrity of cells lacking essential AsmA-like proteins.

Overall, these results demonstrate that the C-terminal hydrophobic α-helices of *P. aeruginosa* YhdP are crucial for its function, in line with what was previously reported for *E. coli* YhdP (Cooper et al., 2025).

2.2 | Fusion with YhdP C-terminal region enhances YdbH activity

Molecular dynamics simulations with the *E. coli* YhdP protein suggested that its C-terminus may interact with the OM and that the C-terminal hydrophobic helices can insert into the inner leaflet of the bilayer (Cooper et al., 2025). Based on this prediction, one could hypothesize that the role of the C-terminal hydrophobic region could be to anchor YhdP to the OM and/or facilitate GPL insertion into the membrane by creating a local perturbation of the inner leaflet. We therefore wondered whether the C-terminal domain of YhdP could provide new functional properties to other AsmA-like proteins and possibly enhance their activity. To this aim, we generated two constructs that express the first 808 residues of YdbH (out of 855) fused to either the YhdP C-terminal domain only (residues 1161–1276) or a longer YhdP C-terminal region (residues 933–1276), resulting in the fusion proteins YdbH-YhdP_short and YdbH-YhdP_long, respectively (Figure 2a,b). The length of YdbH-YhdP_short and YdbH-YhdP_long is comparable to that of YdbH or YhdP, respectively (Table S1). YdbH was chosen for the generation of fusion proteins since its absence has the least impact on OM integrity among AsmA-like proteins likely involved in GPL transport (Ruiz et al., 2021; Sposato et al., 2024), suggesting that it may be less active than other AsmA-like proteins, at least under the conditions tested in previous studies. Moreover, the structure of the AsmA-like domain of YdbH enabled the fusion of the regions of interest of YhdP in a way that preserves a continuity between heterologous β-sheets and maintains the integrity of the hydrophobic groove, according to structural predictions (Figure 2c). Based on the results of molecular dynamics simulations, the two fusion proteins are not expected to experience unfolding or significant alteration in stability or domain organization (Figure S3). Indeed, the radius of gyration and the fraction of native contacts were constant during the simulation time. Also, the number of residues with minimal frustration was much higher than that of highly frustrated residues, suggesting overall stability of the hybrid proteins. Furthermore, the residues close to the fusion point ($-10 < 808 < +10$ residues) were classified as minimally or neutrally frustrated (Figure S3).

To verify their in vivo activity, growth kinetics and vancomycin resistance, used as a proxy for OM

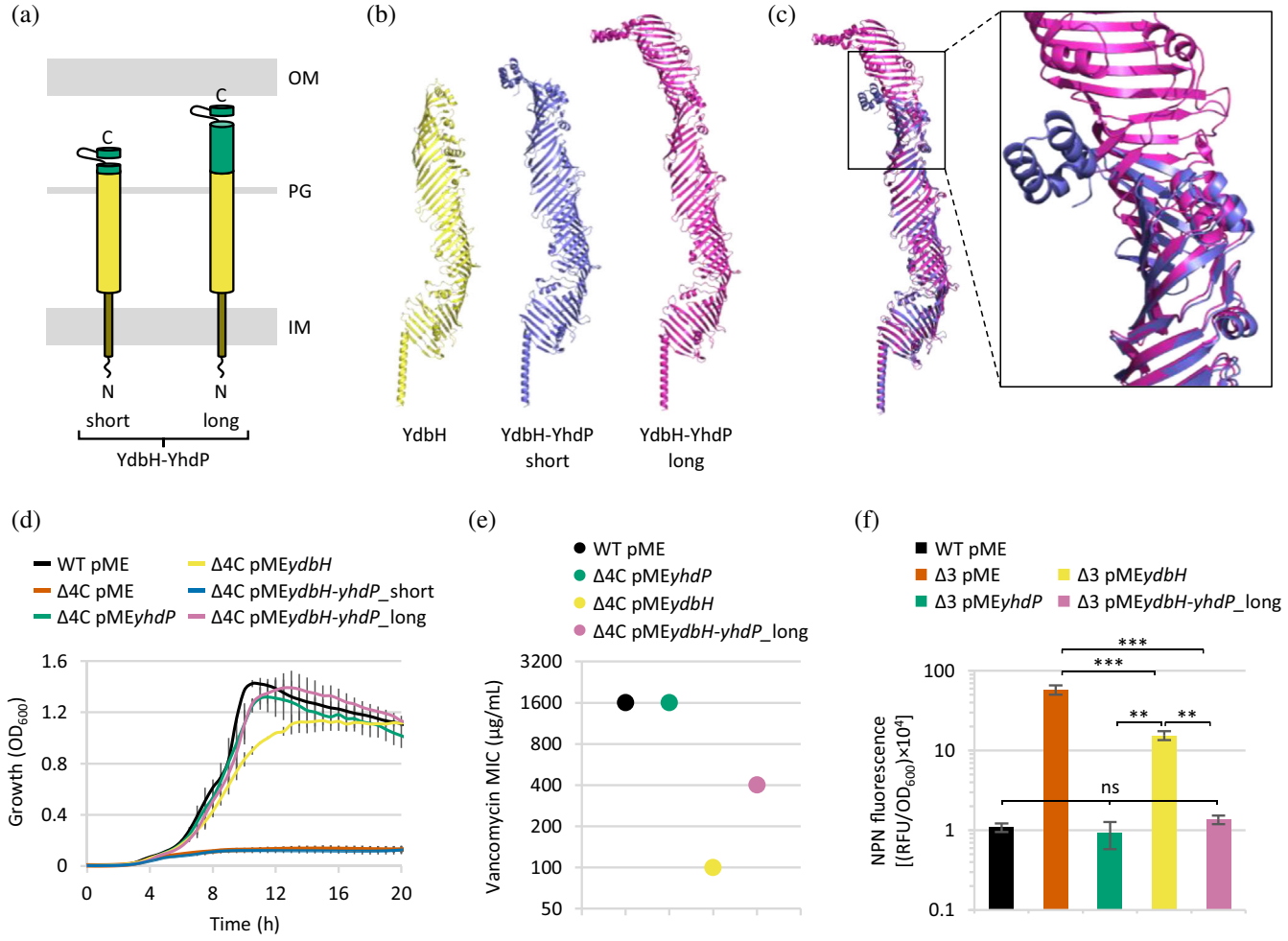

FIGURE 2 (a) Schematic representation of the recombinant fusion proteins YdbH-YhdP_short and YdbH-YhdP_long. (b) Predicted 3D structure of *Pseudomonas aeruginosa* YhdP, YdbH-YhdP_short, and YdbH-YhdP_long. (c) Superimposition of the predicted structures of YdbH-YhdP_short (blue) and YdbH-YhdP_long (purple). The inset highlights the fusion region between YdbH and YhdP domains. (d) Growth curves of *P. aeruginosa* PAO1 (WT) and the conditional mutant Δ*tamB* Δ*yhdP* Δ*ydbH rhaSR*-P_{rhaBAD}::*tamB* ΔPA4735 (Δ4C) carrying the empty plasmid pME6032 (pME) or its derivatives for IPTG-inducible expression of YhdP, YdbH, YdbH-YhdP_short, or YdbH-YhdP_long, cultured in MH supplemented with 16 μM IPTG. Growth curves of the same strains at different IPTG concentrations are shown in Figure S4. (e) Vancomycin MIC for the conditional mutant Δ4C expressing YhdP, YdbH, or YdbH-YhdP_long, cultured in MH supplemented with 16 μM IPTG. The WT strain carrying the empty plasmid was used as positive control. (f) NPN-mediated fluorescence of WT and triple mutant Δ*tamB* Δ*yhdP* Δ*ydbH* (Δ3) cells carrying pME or its derivatives for expression of YhdP, YdbH, or YdbH-YhdP_long, cultured in MH supplemented with 16 μM IPTG. Data in panels d and f are the mean (±standard deviation) of three independent experiments. The asterisks indicate the statistically significant differences between strains of interest (**$p < 0.01$; ***$p < 0.001$; ns, not significant) (ANOVA). Values in panel E represent the mode of at least three independent experiments. IM, inner membrane; OM, outer membrane; PG, peptidoglycan.

integrity, were compared in the rhamnose-dependent conditional mutant Δ*tamB* Δ*yhdP* Δ*ydbH rhaSR*-P_{rhaBAD}::*tamB* ΔPA4735 alternatively expressing the fusion proteins YdbH-YhdP_short or YdbH-YhdP_long, or the wild-type proteins YhdP or YdbH from the same backbone plasmid. As shown in Figure 2d, YdbH-YhdP_short did not restore growth in the absence of rhamnose, while YdbH-YhdP_long promoted growth at levels comparable to the wild-type protein YhdP. Moreover, both YhdP and YdbH-YhdP_long appeared more efficient than YdbH in growth promotion (Figure 2d), suggesting that the fusion with the YhdP C-terminal domain enhanced the ability of YdbH to carry out the essential function exerted by AsmA-like proteins, plausibly the transport of GPLs to the OM. This was confirmed by vancomycin minimum inhibitory concentration (MIC) assay, which revealed that the expression of YdbH-YhdP_long conferred fourfold higher vancomycin resistance than wild-type YdbH, even if it was not able to restore resistance at the level of the wild-type strain or the YhdP expressing conditional mutant (Figure 2e). The lack of functional complementation by YdbH-YhdP_short is consistent with structural predictions suggesting that it cannot span the periplasmic

space. Nonetheless, since we were unable to evaluate the expression levels of the different constructs, the possibility that reduced expression or stability in vivo may have contributed to this outcome cannot be excluded.

To further investigate the effect of fusion proteins on OM integrity, the different proteins were expressed in the triple mutant Δ*tamB* Δ*yhdP* Δ*ydbH* and an *N*-phenyl-1-naphthylamine (NPN) permeability assay was performed. NPN is a hydrophobic probe commonly used to measure OM destabilization, as its fluorescence strongly increases upon binding to membrane lipids (Kwon et al., 2019; Sposato et al., 2024). The triple mutant was used for this assay because it carries the PA4735 gene and can therefore grow even without ectopically expressed proteins, thus allowing OM integrity to be assessed relative to the empty plasmid control. Expression of YhdP and YdbH-YhdP_long completely restored OM integrity in the Δ*tamB* Δ*yhdP* Δ*ydbH* mutant, as NPN fluorescence was comparable to that of the wild-type strain (Figure 2f). Although YdbH expression significantly reduced NPN permeability with respect to the empty plasmid control, the OM of YdbH-expressing cells was still about 10-fold more permeable than that of cells expressing YdbH-YhdP_long (Figure 2f). This result confirmed that YdbH-YhdP_long is more efficient than the wild-type protein YdbH in maintaining OM integrity. Notably, no significant difference was observed in this assay between cells expressing YhdP or YdbH-YhdP_long, in contrast to what was previously noted for vancomycin resistance in the conditional mutant (Figure 2e). This is likely due to the presence of PA4735 in the triple mutant, which could compensate for the slightly lower activity of YdbH-YhdP_long compared to YhdP.

2.3 | Fusion with YhdP C-terminal region makes YdbH independent of its protein partner YnbE

Recently, the OM lipoprotein YnbE was found to be required for YdbH activity in *E. coli*, by interacting with the last β strand of YdbH and extending its hydrophobic groove (Kumar et al., 2024). We hypothesized that fusing YdbH to the C-terminal domain of YhdP could enable YdbH to function independently of YnbE. To prove this hypothesis, we first verified whether YnbE is also crucial for YdbH functionality in *P. aeruginosa*. The YnbE orthologue of *P. aeruginosa* PAO1 is encoded by the PA5306 gene, adjacent to *ydbH* (PA5307), and shares 49.1% identity with *E. coli* YnbE. Thus, we deleted PA5306 in the double mutant Δ*tamB* Δ*yhdP* and compared the growth profile of the resulting strain (Δ*tamB* Δ*yhdP* Δ*ynbE*) to that of the triple mutant Δ*tamB* Δ*yhdP* Δ*ydbH*. If *ynbE* is essential for YdbH functionality also in *P. aeruginosa*, then the absence of YnbE should impair growth and OM integrity to a similar extent as the absence of YdbH. As expected, the deletion of *ynbE* in cells lacking TamB and YhdP caused marked growth defects and increased SDS/EDTA and vancomycin sensitivity (Figure 3a,b), suggestive of relevant OM destabilization. However, *ydbH* deletion had more severe effects on growth and OM integrity than *ynbE* deletion, leading to the hypothesis that YdbH may retain some residual activity in YnbE-deficient cells. Notably, *ynbE* deletion in the wild-type strain did not affect growth and OM functionality (Figure 3a,b). This implies that YnbE function is specifically required in cells that strongly rely on YdbH for growth, as previously observed in *E. coli* (Kumar et al., 2024). Overall, this preliminary experiment confirmed that YdbH needs YnbE for its function also in *P. aeruginosa*.

Then, we ectopically expressed the fusion protein YdbH-YhdP_long in the triple mutant Δ*tamB* Δ*yhdP* Δ*ynbE* to verify whether it was able to promote growth also in YnbE-deficient cells. YdbH-YhdP_long fully restored the growth of Δ*tamB* Δ*yhdP* Δ*ynbE* cells to wild-type levels (Figure 3c), indicating that this fusion protein does not require YnbE to accomplish its essential function. In contrast, the expression of YdbH-YhdP_short in the same mutant was unable to promote growth (Figure 3c), further suggesting that this fusion protein is inactive.

Remarkably, also ectopic expression of wild-type YdbH failed to support growth of the mutant Δ*tamB* Δ*yhdP* Δ*ynbE*, which already expresses YdbH at physiological levels from the chromosomal gene (Figure 3c). This result was unexpected, as deletion experiments suggested that YdbH likely retains some activity in the absence of YnbE (Figure 3a,b), leading us to assume that YdbH overexpression could have provided some benefit. The lack of any growth promoting effect upon YdbH overexpression might be explained by the involvement of additional OM partner(s) beyond YnbE, which may be already saturated by the YdbH levels expressed by the chromosomal gene. This hypothesis would align with structural predictions indicating that the YdbH–YnbE complex is still too short to bridge the entire periplasm (Kumar et al., 2024). At present, the only AsmA-like protein for which an integral OM partner that could assist GPL insertion into the OM has been identified is TamB (Kumar & Ruiz, 2023; Ruiz et al., 2021; Sposato et al., 2024), which interacts with TamA, a β-barrel protein of the Omp85 family (Selkrig et al., 2015). Although recently proposed to participate in GPL insertion into the OM (Douglass et al., 2022; Rai et al., 2024; Ruiz et al., 2021; Sposato et al., 2024), the TamB-TamA complex was originally implicated in the assembly of a subset of OM β-barrel proteins (Stubenrauch & Lithgow, 2019), and its possible dual role in protein and/or GPL transport remains under debate (Goh et al., 2024; Wang et al., 2024). We have previously shown that *tamA* deletion has no effect on *P. aeruginosa* growth, suggesting that TamA is not required for the activity of all essential AsmA-like

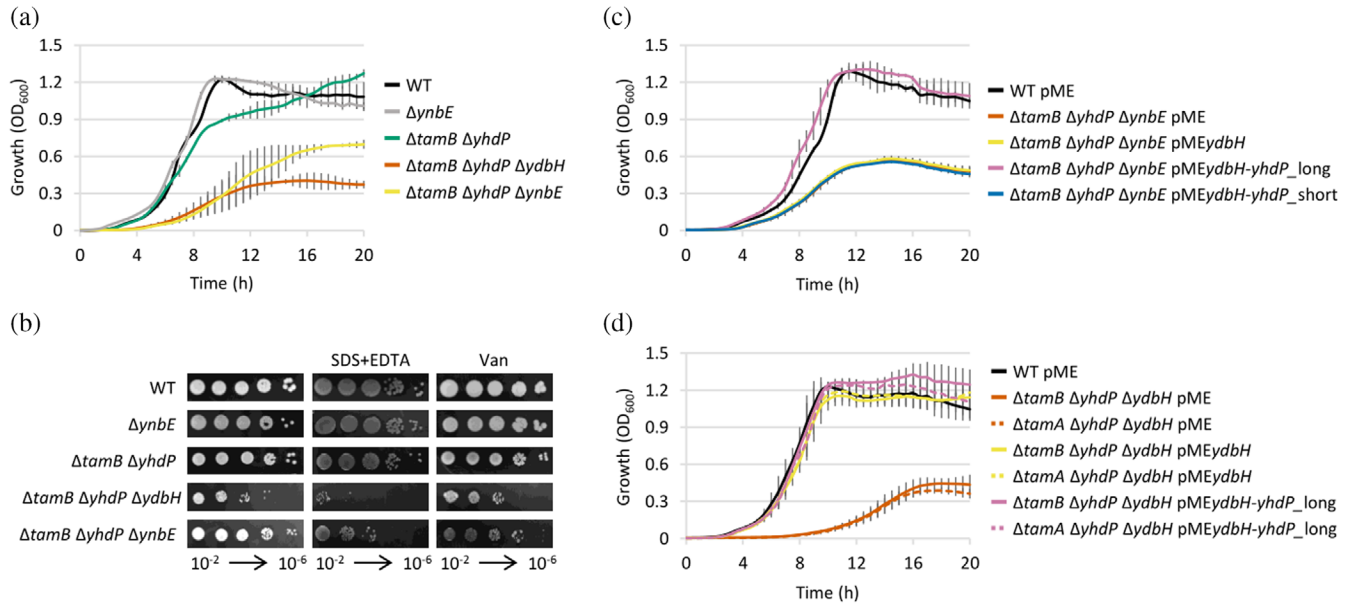

FIGURE 3 (a) Growth curves of the wild-type strain *Pseudomonas aeruginosa* PAO1 (WT) and the isogenic mutants Δ*ynbE*, Δ*tamB* Δ*yhdP*, Δ*tamB* Δ*yhdP* Δ*ydbH*, and Δ*tamB* Δ*yhdP* Δ*ynbE*, cultured in MH. (b) Plating efficiency of the same strains described in panel A on MH agar plates supplemented or not with 0.25% SDS and 0.25 mM EDTA (SDS + EDTA) or 10 μg/mL vancomycin (Van). (c) Growth curves of the WT strain and the triple mutant Δ*tamB* Δ*yhdP* Δ*ynbE* carrying the empty plasmid pME6032 (pME) or its derivatives for IPTG-inducible expression of YdbH, YdbH-YhdP_long, or YdbH-YhdP_short, cultured in MH supplemented with 16 μM IPTG. Growth curves of the same strains at different IPTG concentrations are shown in Figure S5. (d) Growth curves of the WT strain and the triple mutants Δ*tamB* Δ*yhdP* Δ*ydbH* and Δ*tamA* Δ*yhdP* Δ*ydbH* carrying the empty plasmid pME or its derivatives for IPTG-inducible expression of YdbH or YdbH-YhdP_long, cultured in MH supplemented with 16 μM IPTG. Growth curves of the same strains at different IPTG concentrations are shown in Figure S6. Data in panels a, c, and d are the mean (±standard deviation) of three independent experiments. Images in panel B are representative of three independent experiments.

proteins (Sposato et al., 2024). However, this evidence does not rule out a possible contribution of TamA in YdbH function, as YdbH inactivation per se has negligible effects on growth and OM integrity (Sposato et al., 2024). To conclusively determine whether TamA contributes to GPL insertion mediated by YdbH, here we ectopically expressed YdbH, and the fusion protein YdbH-YhdP_long as control, in the triple mutant Δ*tamA* Δ*yhdP* Δ*ydbH*, which lacks TamA and displays severely compromised growth due to the simultaneous inactivation of TamB and absence of YhdP and YdbH (Figure 3d) (Sposato et al., 2024). Notably, YdbH expression fully restored the growth of the mutant even in the absence of TamA, and the same result was obtained with YdbH-YhdP_long (Figure 3d). Such results rule out that TamA is required for YdbH function and, thus, that it may represent an additional component of the YhdP-YnbE complex.

2.4 | YhdP and YdbH fused to the YhdP C-terminal region function in a heterologous host

Our data demonstrated that fusing YdbH to the C-terminal region of YhdP bypasses the requirement for YdbH protein partner(s) (Figure 3) and enhances the protein ability to promote growth and support OM biogenesis compared to the YdbH native protein (Figure 2). Based on molecular dynamics simulations, Cooper et al. proposed that the C-terminal hydrophobic helices of *E. coli* YhdP insert into the periplasmic leaflet of the OM (Cooper et al., 2025). However, it remains unclear whether these helices could promote GPL insertion into the membrane, possibly through perturbation of the GPL leaflet continuity, or if this process requires a yet-unidentified YhdP OM partner.

We reasoned that initial insights to address this issue could be gained by examining protein behavior in a heterologous host. Indeed, the YhdP orthologues from *E. coli* and *P. aeruginosa* share very low amino acid identity (Sposato et al., 2024), with only 26.7% identity in the final 90 residues including the hydrophobic C-terminal region. This is suggestive of poor conservation of putative interacting residues and, consequently, of only weak or inefficient interaction between the *P. aeruginosa* protein and potential non-native partners in *E. coli* (Lewis et al., 2012; Mika & Rost, 2006). We therefore ectopically expressed all *P. aeruginosa* protein variants investigated in this study in the *E. coli* mutant Δ*tamB* Δ*yhdP*, which is characterized by impaired growth and hypersensitivity to vancomycin (Figure 4, Figure S7), indicative of OM integrity defects (Ruiz et al., 2021).

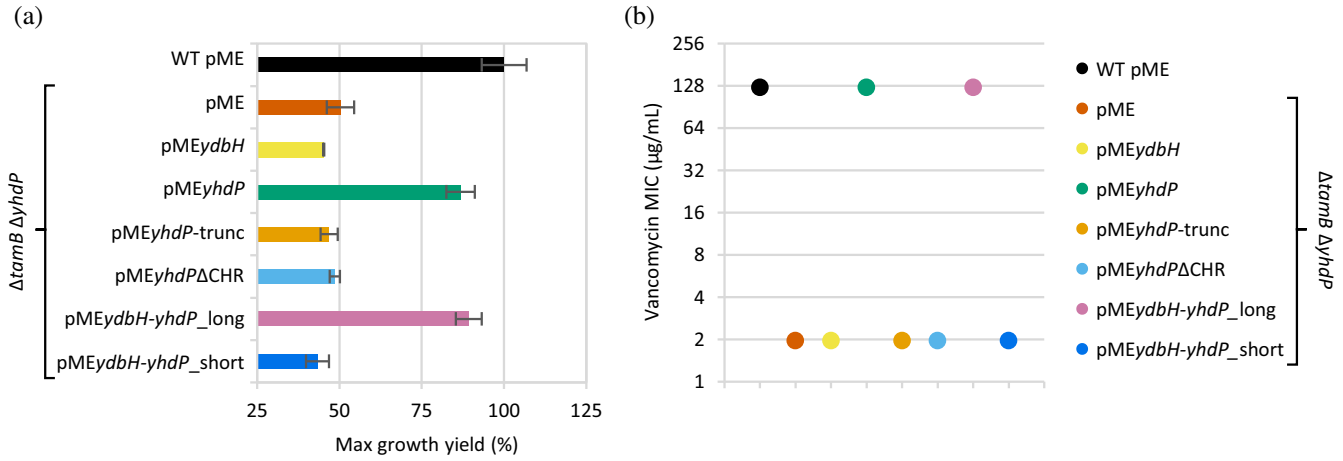

FIGURE 4 (a) Maximum growth yields and (b) vancomycin MIC for the *Escherichia coli* wild-type strain MG1655 (WT) and the isogenic mutant Δ*tamB* Δ*yhdP* carrying the empty plasmid pME6032 (pME) or its derivatives for IPTG-inducible expression of the *Pseudomonas aeruginosa* proteins YdbH, YhdP, or their variants YhdP-trunc, YhdPΔCHR, YdbH-YhdP_long, or YdbH-YhdP_short, cultured in MH supplemented with an optimal concentration of IPTG (depending on the strain, see Figure S7 for details). Values in panel a are expressed as percentages with respect to the maximum growth yields of WT pME and correspond to the mean (±standard deviation) of three independent experiments. Growth curves of the same strains at different IPTG concentrations are shown in Figure S7. Values in panel b represent the mode of at least three independent experiments.

Interestingly, both *P. aeruginosa* YhdP and the fusion protein YdbH-YhdP_long restored growth and vancomycin resistance to (almost) wild-type levels, while all other proteins did not display any rescue effect (Figure 4, Figure S7). The inability of *P. aeruginosa* YdbH to complement the *E. coli* mutant can be attributed either to inefficient interaction with the *E. coli* YdbH partner(s), as YdbH orthologues also share very low homology (24.4% identity over only one sixth of the proteins) (Sposato et al., 2024), or to the fact that Δ*tamB* Δ*yhdP* cells express the endogenous YdbH protein, which might saturate YnbE and thereby render the *P. aeruginosa* orthologue inactive. Either way, these results further confirm that the C-terminal region of YhdP confers new functions to YdbH, including the ability to work in the heterologous host *E. coli*. While this interspecies complementation assay supports the hypothesis that the YhdP C-terminal region may have intrinsic properties that allow OM interaction and GPL insertion, this remains to be confirmed through biochemical and biophysical analyses.

3 | CONCLUSIONS

In this study we demonstrated that the C-terminal hydrophobic α-helices of *P. aeruginosa* YhdP are crucial for its function in maintaining OM integrity, likely by enabling membrane interaction and/or facilitating GPL insertion. This aligns with what was recently reported for the *E. coli* orthologue (Cooper et al., 2025), suggesting that this structural and functional feature of YhdP may be conserved across different species. In addition, we found that also in *P. aeruginosa* the function of YdbH relies on the OM lipoprotein YnbE, recently identified as a YdbH protein partner in *E. coli* (Kumar et al., 2024). Most importantly, not only does the deletion of the C-terminal hydrophobic region impair YhdP functionality, but its fusion to YdbH also enhances YdbH activity and makes it independent of its OM partner YnbE, provided that the fusion protein is long enough to span the entire periplasmic space. Furthermore, both *P. aeruginosa* YhdP and the fusion protein YdbH-YhdP_long proved to be active in the heterologous host *E. coli*, reinforcing the notion that the C-terminal hydrophobic region of YhdP may possess intrinsic, transferable properties that support the essential function played by AsmA-like proteins in Gram-negative bacteria. Overall, these results are consistent with a model in which the hydrophobic C-terminus of YhdP facilitates interaction with the OM, possibly enabling GPL delivery in the absence of additional protein partners. The presence of this hydrophobic C-terminal region, along with the protein length compatible with a transmembrane periplasmic bridge (Cooper et al., 2025; Kumar & Ruiz, 2023), could therefore explain the more prominent role of YhdP in maintaining OM homeostasis compared to other AsmA-like proteins (Douglass et al., 2022; Ruiz et al., 2021; Sposato et al., 2024). However, structural and biophysical studies will be needed to confirm this hypothesis and dissect the molecular basis of GPL insertion into the OM mediated by YhdP and other AsmA-like proteins.

Our findings also offer insights into the modularity and mechanistic versatility of AsmA-like proteins, as evidenced by the finding that the expression of the YdbH-YhdP_long fusion protein essentially phenocopied the

wild-type protein YhdP, both in *P. aeruginosa* and in the heterologous host *E. coli*. Recently, Rai and colleagues reported genetic evidence suggesting that different AsmA-like proteins may have different GPL substrate transport preferences (Rai et al., 2024), presumably due to the N-terminal regions that interact with the IM. However, we observed that the expression of YhdP or YdbH-YhdP_long alone can restore wild-type levels of growth and OM integrity in a mutant deficient in all other essential AsmA-like proteins. While this result does not exclude the possibility of different substrate preferences, it implies that a single protein, either YhdP or YdbH fused to the C-terminal YhdP domain, is sufficient to supply the OM with all GPL species required for normal membrane functionality. This suggests that at least some AsmA-like proteins may be rather promiscuous, accommodating and transporting different GPL types. In vitro binding assays with purified proteins will be crucial not only to validate this hypothesis but also to uncover the molecular determinants of substrate specificity in this fascinating class of bacterial transport proteins.

4 | MATERIALS AND METHODS

4.1 | Bacterial strains, plasmids, and growth conditions

Strains and plasmids used in this study are listed in Tables S2 and S3, respectively. Bacteria were routinely cultured in Lysogeny broth, Lennox formulation (LB) for genetic manipulation. Mueller Hinton broth (MH) was used for plate efficiency, growth, MIC, and permeability assays. When required, antibiotics were added at the following concentrations for *E. coli* (the concentrations used for *P. aeruginosa* are shown in brackets): ampicillin, 100 μg/mL; tetracycline, 10 μg/mL (25–100 μg/mL); nalidixic acid, 15 μg/mL; chloramphenicol, 30 μg/mL (375 μg/mL).

4.2 | Generation of plasmids and mutant strains

To obtain the constructs for the in-frame deletion of a 78-bp region in the *yhdP* coding sequence encoding the C-terminal hydrophobic residues (aa 1216–1241) of YhdP, two DNA fragments of approximately 500 bp each, encompassing the upstream (↑) and downstream (↓) regions of the *yhdP* CHR coding sequence, were PCR-amplified, directionally cloned into pBluescript II KS (pBS; Table S3), and verified by DNA sequencing. Then, the ↑↓ fragment was excised from pBS and sub-cloned into the *sacB*-based suicide vector pDM4 (Milton et al., 1996). The resulting construct pDM4*yhdP*CHR↑↓ was transferred into the *P. aeruginosa* mutant Δ*tamB* Δ*ydbH* by conjugation, and transconjugants were selected on LB agar plates containing 15 μg/mL nalidixic acid and 375 μg/mL chloramphenicol. The deletion mutant was obtained by homologous recombination and sucrose-based selection as previously described (Lo Sciuto et al., 2022), and verified by PCR and DNA sequencing.

The same strategy was employed to obtain deletion mutants in the *ynbE* (PA5306) gene, by generating the construct pDM4*ynbE*↑↓ (Table S3), introducing it into the *P. aeruginosa* strains PAO1 and Δ*tamB* Δ*yhdP*, and selecting the *ynbE* deletion mutants as described above.

To generate the plasmid pME*yhdP*-trunc, the coding sequence of *yhdP* corresponding to residues 1–1219 was amplified by PCR, using the genomic DNA of the PAO1 as the template. To generate the plasmid pME*yhdP*ΔCHR, the entire coding sequence of the *yhdP*ΔCHR allele was amplified by PCR, using the genomic DNA of the Δ*tamB* Δ*ydbH* *yhdP*ΔCHR mutant as the template. The amplicons were individually cloned into the shuttle vector pME6032 (Heeb et al., 2002), under the control of an IPTG-inducible promoter, and verified by DNA sequencing.

For the construction of the plasmids for the expression of the YdbH-YhdP fusion proteins, the DNA region encoding the residues 1–808 of YdbH was amplified by PCR from the genomic DNA of PAO1 and cloned into pBS, yielding pBS*ydbH*$_{1\text{-}808}$ (Table S3). Then, two DNA regions encoding either the residues 1161–1276 or the residues 933–1276 of YhdP were PCR-amplified from the genomic DNA of PAO1 and individually cloned into pBS*ydbH*$_{1\text{-}808}$, resulting in pBS*ydbH-yhdP*_short and pBS*ydbH yhdP*_long, respectively (Table S3), which were verified by DNA sequencing. Finally, the DNA fragments *ydbH-yhdP*_short and pBS*ydbH yhdP*_long were excised from the pBS derivatives and subcloned into pME6032 under the control of the IPTG-inducible promoter, yielding pME*ydbH-yhdP*_short and pME*ydbH yhdP*_long, respectively (Table S3).

All primers and restriction enzymes used for PCR and cloning are listed in Table S4.

4.3 | Plating efficiency and growth assays

For plating efficiency assays, bacterial strains were cultured in MH, supplemented with 0.01% rhamnose for the conditional mutants, harvested by centrifugation, and resuspended in sterile saline solution at $OD_{600} = 1$. Serial 10-fold dilutions were prepared and 5 μL aliquots of selected dilutions were spotted onto MH agar plates supplemented or not with either 0.25% SDS and 0.25 mM EDTA or vancomycin at 100 or 10 μg/mL, as indicated.

For planktonic growth assays, bacterial strains were precultured in MH, supplemented with 0.01% rhamnose for the conditional mutants, and then refreshed 1:1000

in MH in the absence or presence of rhamnose or IPTG at the indicated concentrations. Bacterial cultures were incubated in 96-well microtiter plates (200 μL in each well) at 37°C in a Tecan Spark 10 M microtiter plate reader, and growth was measured over time as the optical density at 600 nm (OD_{600}) of the bacterial cultures. Maximum growth yields were determined by calculating the ratio of the maximum OD_{600} values, expressed as a percentage relative to the control strain, as indicated in the figure legends.

4.4 | Membrane permeability assays

Bacterial strains were cultured in MH, and exponential phase cells were harvested by centrifugation and resuspended in 5 mM HEPES (pH 7.2) at $OD_{600} = 3$. Equal volumes (150 μL) of HEPES solution, containing or not 20 μM NPN, and bacterial suspensions were mixed, and 100 μL of each sample was aliquoted on a black flat bottom 96-well plate. OD_{600} and fluorescence (excitation at 350 nm and emission at 420 nm) were measured in a Tecan Spark 10 M microtiter plate reader after a 2-min incubation at room temperature, subtracted of the background values of samples without NPN, and normalized to the OD_{600} of the cell suspension (Cervoni et al., 2021).

4.5 | MIC assays

The MIC of vancomycin was determined through the broth microdilution method. Strains carrying pME6032 or its derivatives were precultured in MH, supplemented with tetracycline at 10 or 25 μg/mL (for *E. coli* and *P. aeruginosa*, respectively) and 0.01% rhamnose for the *P. aeruginosa* conditional mutants, and refreshed at ca. 5×10^5 cells/mL in MH in the presence of the indicated IPTG concentrations and increasing concentrations of vancomycin. MIC was recorded after 24 h at 37°C.

4.6 | Bioinformatic analyses and molecular dynamics simulations

TMHs were predicted using the online tool TMHMM 2.0 (https://services.healthtech.dtu.dk/services/TMHMM-2.0/) (Krogh et al., 2001). The predicted structures of YhdP (PA4476) and YdbH (PA5307) were downloaded from AlphaFold (Q9HVU5 YhdP 9828 atoms; Q9HTP7 YdbH 6579 atoms). Classical molecular dynamics simulations of 500 ns were performed to relax the systems; then the last frame was used as the initial structure for the following molecular dynamics simulations. The models were built with Maestro Schrodinger (Schrödinger Release 2023–4: Maestro, Schrödinger, LLC, New York, NY, 2023), then translated into coarse grain using the martinize script (de Jong et al., 2013) and embedded in a membrane bilayer simulating the IM composed of 70% of 1-palmitoyl-2-oleoyl-phosphatidylethanolamine (POPE) and 30% of 1-palmitoyl-2-oleoyl-glycero-3-phosphocholine (POPC). The insane.py script (Wassenaar et al., 2015) was used to create a membrane environment around these structures. YhdP and YdbH-YhdP_long were modeled with the inner leaflet of the OM at the C-terminus and the outer leaflet of the IM at the N-terminus; all the other studied proteins were modeled only with the outer leaflet of the IM. All simulations were performed within a charge neutralized system with the addition of ions corresponding to a 0.15 M NaCl solution. The models featured around 3 hundred thousand atoms including water and ions. All molecular dynamics simulations were performed using GROMACS 2024.1 (Abraham et al., 2015). Martini v3.0 (Souza et al., 2021) was used as the force field with an elastic network. The system was minimized using a steep integrator with a maximum number of 500,000 steps to perform. An npt equilibration of 5,000,000 nsteps was performed after minimization, with constant temperature of 300 K using a velocity rescale thermostat; also, the pressure was held at 1 bar by using a Berensen barostat with a relaxation time of 4 ps. Then all systems were subjected to simulations for 1 μs each and replicated three times to ensure reproducibility. The simulations were converted into all-atomistic simulations using the cg2all script (Heo & Feig, 2024) to gain insights into the structural differences induced by the chimeric modifications and to obtain all atomistic structure for the frustratometer analysis. MDAnalysis was used for the calculation of the radius of gyration and the fraction of native contacts (Michaud-Agrawal et al., 2011). Graphs were generated with Matplotlib (Hunter, 2007) and pictures were created with the PyMOL Molecular Graphics System, Version 2.0 (Schrödinger, LLC). The FrustratometeR package was used to calculate the frustration of the protein structures during the simulations (Rausch et al., 2021). This method of measuring frustration assumes that the residues are not only changed in identity but also displaced in position. A local frustration index is defined as the *Z*-score (0.78) of the free energy of parts of the native structure with respect to the distribution of the energy of rearranged decoys. If a native pair of interacting residues has an energy that lies in the most favorable end of the distribution (>0.78), the interaction is labeled as minimally frustrated; if the energy of the residues pair lies in the most unfavorable end of the distribution (<−1), the interaction is labeled as highly frustrated; if the energy of the residues pair lies in the range between 0.78 and −1, it is labeled as neutral (Ferreiro et al., 2018).

4.7 | Statistical analysis

Statistical analysis was performed with the software GraphPad Instat, using the ANOVA with Tukey's multiple comparisons test.

AUTHOR CONTRIBUTIONS

Davide Sposato: Conceptualization; methodology; data curation; investigation; validation; visualization; writing – original draft; writing – review and editing. **Camilla Pederzoli:** Investigation; validation; writing – review and editing. **Marianna Bufano:** Methodology; investigation; validation; visualization; writing – original draft; data curation; writing – review and editing. **Pietro Sciò:** Investigation; validation; writing – review and editing. **Ludovica Rossi:** Investigation; validation; writing – review and editing. **Livia Leoni:** Funding acquisition; writing – review and editing; visualization. **Giordano Rampioni:** Writing – review and editing; data curation; visualization; funding acquisition. **Paolo Visca:** Visualization; writing – review and editing; project administration. **Antonio Coluccia:** Supervision; conceptualization; methodology; data curation; visualization; funding acquisition; writing – original draft; writing – review and editing; resources. **Francesco Imperi:** Writing – original draft; writing – review and editing; funding acquisition; supervision; resources; project administration; conceptualization; methodology; data curation.

ACKNOWLEDGMENTS

We thank Prof. Natividad Ruiz for kindly providing us with the *E. coli* mutant Δ*tamB* Δ*yhdP*. This work was supported by the Italian Ministry of University and Research (MUR) with the grants Excellence Departments (art. 1, commi 314-337 Legge 232/2016) to the Department of Science of the University Roma Tre, PRIN 2020 (20208LLXEJ to FI and AC), and PRIN 2022 (20224BYR59 to GR and 2022C5PNXB to LL). The authors also acknowledge the support of NBFC (MUR PNRR, Project CN00000033) and Rome Technopole (F83B22000040006) to the Department of Science of the University Roma Tre. AC would like to acknowledge the support of the Italian Cystic Fibrosis Research Foundation (grant FFC#6/2023). AC, MB, and PS acknowledge the CINECA award under the ISCRA initiative, for the availability of high-performance computing resources and support. The funders had no role in study design, data collection and interpretation, or the decision to submit the work for publication. Open access funding provided by BIBLIOSAN.

DATA AVAILABILITY STATEMENT

The data that support the findings of this study are available from the corresponding author upon reasonable request.

ORCID

Francesco Imperi https://orcid.org/0000-0001-5080-5665

REFERENCES

Abraham MJ, Murtola T, Schulz R, Páll S, Smith JC, Hess B, et al. GROMACS: high performance molecular simulations through multi-level parallelism from laptops to supercomputers. SoftwareX. 2015;1–2:19–25.

Best RB, Hummer G, Eaton WA. Native contacts determine protein folding mechanisms in atomistic simulations. Proc Natl Acad Sci USA. 2013;110:17874–9.

Cervoni M, Lo Sciuto A, Bianchini C, Mancone C, Imperi F. Exogenous and endogenous phosphoethanolamine transferases differently affect colistin resistance and fitness in *Pseudomonas aeruginosa*. Front Microbiol. 2021;12:778968.

Choi U, Lee CR. Antimicrobial agents that inhibit the outer membrane assembly machines of Gram-negative bacteria. J Microbiol Biotechnol. 2019;29:1–10.

Cooper BF, Clark R, Kudhail A, Dunn D, Tian Q, Bhabha G, et al. Phospholipid transport across the bacterial periplasm through the envelope-spanning bridge YhdP. J Mol Biol. 2025;437:168891.

de Jong DH, Singh G, Bennett WF, Arnarez C, Wassenaar TA, Schäfer LV, et al. Improved parameters for the martini coarse-grained protein force field. J Chem Theory Comput. 2013;9:687–97.

Dong H, Tang X, Zhang Z, Dong C. Structural insight into lipopolysaccharide transport from the Gram-negative bacterial inner membrane to the outer membrane. Biochim Biophys Acta Mol Cell Biol Lipids. 2017;1862:1461–7.

Douglass MV, McLean AB, Trent MS. Absence of YhdP, TamB, and YdbH leads to defects in glycerophospholipid transport and cell morphology in Gram-negative bacteria. PLoS Genet. 2022;18:e1010096.

Ferreiro DU, Komives EA, Wolynes PG. Frustration, function and folding. Curr Opin Struct Biol. 2018;48:68–73.

Goh KJ, Stubenrauch CJ, Lithgow T. The TAM, a translocation and assembly module for protein assembly and potential conduit for phospholipid transfer. EMBO Rep. 2024;25:1711–20.

Grimm J, Shi H, Wang W, Mitchell AM, Wingreen NS, Huang KC, et al. The inner membrane protein YhdP modulates the rate of anterograde phospholipid flow in *Escherichia coli*. Proc Natl Acad Sci U S A. 2020;117:26907–14.

Heeb S, Blumer C, Haas D. Regulatory RNA as mediator in GacA/RsmA-dependent global control of exoproduct formation in *Pseudomonas fluorescens* CHA0. J Bacteriol. 2002;184:1046–56.

Henderson JC, Zimmerman SM, Crofts AA, Boll JM, Kuhns LG, Herrera CM, et al. The power of asymmetry: architecture and assembly of the gram-negative outer membrane lipid bilayer. Annu Rev Microbiol. 2016;70:255–78.

Heo L, Feig M. One bead per residue can describe all-atom protein structures. Structure. 2024;32:97–111.e6.

Hicks G, Jia Z. Structural basis for the lipopolysaccharide export activity of the bacterial lipopolysaccharide transport system. Int J Mol Sci. 2018;19:2680.

Hunter JD. Matplotlib: a 2D graphics environment. Comput Sci Eng. 2007;9:90–5.

Joshi SY, Deshmukh SA. A review of advancements in coarse-grained molecular dynamics simulations. Mol Simul. 2021;47:10–1.

Krogh A, Larsson B, von Heijne G, Sonnhammer EL. Predicting transmembrane protein topology with a hidden Markov model: application to complete genomes. J Mol Biol. 2001;305:567–80.

Kumar S, Davis RM, Ruiz N. YdbH and YnbE form an intermembrane bridge to maintain lipid homeostasis in the outer membrane of

Escherichia coli. Proc Natl Acad Sci USA. 2024;121: e2321512121.
Kumar S, Ruiz N. Bacterial AsmA-like proteins: bridging the gap in intermembrane phospholipid transport. Contact (Thousand Oaks). 2023;6:25152564231185931.
Kwon JY, Kim MK, Mereuta L, Seo CH, Luchian T, Park Y. Mechanism of action of antimicrobial peptide P5 truncations against *Pseudomonas aeruginosa* and *Staphylococcus aureus*. AMB Express. 2019;9:122.
Lees JA, Reinisch KM. Inter-organelle lipid transfer: a channel model for Vps13 and chorein-N motif proteins. Curr Opin Cell Biol. 2020;65:66–71.
Lehman KM, Grabowicz M. Countering gram-negative antibiotic resistance: recent progress in disrupting the outer membrane with novel therapeutics. Antibiotics (Basel). 2019;8:163.
Levine TP. Remote homology searches identify bacterial homologues of eukaryotic lipid transfer proteins, including Chorein-N domains in TamB and AsmA and Mdm31p. BMC Mol Cell Biol. 2019; 20:43.
Lewis AC, Jones NS, Porter MA, Deane CM. What evidence is there for the homology of protein-protein interactions? PLoS Comput Biol. 2012;8:e1002645.
Lo Sciuto A, Spinnato MC, Pasqua M, Imperi F. Generation of stable and unmarked conditional mutants in *Pseudomonas aeruginosa*. Methods Mol Biol. 2022;2548:21–35.
Melia TJ, Reinisch KM. A possible role for VPS13-family proteins in bulk lipid transfer, membrane expansion and organelle biogenesis. J Cell Sci. 2022;135:jcs259357.
Michaud-Agrawal N, Denning EJ, Woolf TB, Beckstein O. MDAnalysis: a toolkit for the analysis of molecular dynamics simulations. J Comput Chem. 2011;32:2319–27.
Mika S, Rost B. Protein-protein interactions more conserved within species than across species. PLoS Comput Biol. 2006;2:e79.
Milton DL, O'Toole R, Horstedt P, Wolf-Watz H. Flagellin A is essential for the virulence of *Vibrio anguillarum*. J Bacteriol. 1996;178: 1310–9.
Nikaido H. Molecular basis of bacterial outer membrane permeability revisited. Microbiol Mol Biol Rev. 2003;67:593–656.
Okuda S, Sherman DJ, Silhavy TJ, Ruiz N, Kahne D. Lipopolysaccharide transport and assembly at the outer membrane: the PEZ model. Nat Rev Microbiol. 2016;14:337–45.
Onuchic JN, Luthey-Schulten Z, Wolynes PG. Theory of protein folding: the energy landscape perspective. Annu Rev Phys Chem. 1997;48:545–600.
Plummer AM, Fleming KG. From chaperones to the membrane with a BAM! Trends Biochem Sci. 2016;41:872–82.
Rai AK, Sawasato K, Bennett HC, Kozlova A, Sparagna GC, Bogdanov M, et al. Genetic evidence for functional diversification of gram-negative intermembrane phospholipid transporters. PLoS Genet. 2024;20:e1011335.
Rausch AO, Freiberger MI, Leonetti CO, Luna DM, Radusky LG, Wolynes PG, et al. FrustratometeR: an R-package to compute local frustration in protein structures, point mutants and MD simulations. Bioinformatics. 2021;37:3038–40.
Ruiz N, Davis RM, Kumar S. YhdP, TamB, and YdbH are redundant but essential for growth and lipid homeostasis of the Gram-negative outer membrane. MBio. 2021;12(6):e0271421.
Selkrig J, Belousoff MJ, Headey SJ, Heinz E, Shiota T, Shen HH, et al. Conserved features in TamA enable interaction with TamB to drive the activity of the translocation and assembly module. Sci Rep. 2015;5:12905.
Silhavy TJ, Kahne D, Walker S. The bacterial cell envelope. Cold Spring Harb Perspect Biol. 2010;2:a000414.
Souza PCT, Alessandri R, Barnoud J, Thallmair S, Faustino I, Grünewald F, et al. Martini 3: a general purpose force field for coarse-grained molecular dynamics. Nat Methods. 2021;18:382–8.
Sperandeo P, Martorana AM, Polissi A. Lipopolysaccharide biosynthesis and transport to the outer membrane of Gram-negative bacteria. Subcell Biochem. 2019;92:9–37.
Sperandeo P, Martorana AM, Zaccaria M, Polissi A. Targeting the LPS export pathway for the development of novel therapeutics. Biochim Biophys Acta Mol Cell Res. 2023;1870:119406.
Sposato D, Mercolino J, Torrini L, Sperandeo P, Lucidi M, Alegiani R, et al. Redundant essentiality of AsmA-like proteins in *Pseudomonas aeruginosa*. mSphere. 2024;9:e0067723.
Stubenrauch CJ, Lithgow T. The TAM: a translocation and assembly module of the β-barrel assembly machinery in bacterial outer membranes. EcoSal Plus. 2019;8. https://doi.org/10.1128/ecosalplus.ESP-0036-2018
Sun J, Rutherford ST, Silhavy TJ, Huang KC. Physical properties of the bacterial outer membrane. Nat Rev Microbiol. 2022;20:236–48.
Vannimenus J, Toulouse G. Theory of the frustration effect. II. Ising spins on a square lattice. J Phys C Solid State Phys. 1977;10: L537.
Walker SS, Black TA. Are outer-membrane targets the solution for MDR Gram-negative bacteria? Drug Discov Today. 2021;26: 2152–8.
Wang X, Nyenhuis SB, Bernstein HD. The translocation assembly module (TAM) catalyzes the assembly of bacterial outer membrane proteins in vitro. Nat Commun. 2024;15:7246.
Wassenaar TA, Ingólfsson HI, Böckmann RA, Tieleman DP, Marrink SJ. Computational lipidomics with insane: a versatile tool for generating custom membranes for molecular simulations. J Chem Theory Comput. 2015;11:2144–55.
Wesseling CMJ, Martin NI. Synergy by perturbing the gram-negative outer membrane: opening the door for gram-positive specific antibiotics. ACS Infect Dis. 2022;8:1731–57.
Zückert WR. Secretion of bacterial lipoproteins: through the cytoplasmic membrane, the periplasm and beyond. Biochim Biophys Acta. 2014;1843:1509–16.

SUPPORTING INFORMATION

Additional supporting information can be found online in the Supporting Information section at the end of this article.

How to cite this article: Sposato D, Pederzoli C, Bufano M, Sciò P, Rossi L, Leoni L, et al. Structure–function relationship of the *Pseudomonas aeruginosa* AsmA-like proteins YhdP and YdbH involved in outer membrane biogenesis. Protein Science. 2025;34(10): e70227. https://doi.org/10.1002/pro.70227